# Transverse single-spin asymmetry of midrapidity $\pi^0$ and $\eta$ mesons in $p + \mathrm{Au}$ and $p + \mathrm{Al}$ collisions at $\sqrt{s_{NN}} = 200$ GeV


N. J. Abdulameer,[14] U. Acharya,[19] C. Aidala,[40] Y. Akiba,[54,55,†] M. Alfred,[21] V. Andrieux,[40] N. Apadula,[26] H. Asano,[32,54] B. Azmoun,[7] V. Babintsev,[22] N. S. Bandara,[38] K. N. Barish,[8] S. Bathe,[5,55] A. Bazilevsky,[7] M. Beaumier,[8] R. Belmont,[11,47] A. Berdnikov,[57] Y. Berdnikov,[57] L. Bichon,[65] B. Blankenship,[65] D. S. Blau,[31,44] J. S. Bok,[46] V. Borisov,[57] M. L. Brooks,[34] J. Bryslawskyj,[5,8] V. Bumazhnov,[22] S. Campbell,[12] V. Canoa Roman,[60] R. Cervantes,[60] M. Chiu,[7] C. Y. Chi,[12] I. J. Choi,[23] J. B. Choi,[28,*] Z. Citron,[66] M. Connors,[19,55] R. Corliss,[60] Y. Corrales Morales,[34] N. Cronin,[60] M. Csanád,[15] T. Csörgő,[39,67] T. W. Danley,[48] M. S. Daugherity,[1] G. David,[7,60] C. T. Dean,[34] K. DeBlasio,[45] K. Dehmelt,[60] A. Denisov,[22] A. Deshpande,[55,60] E. J. Desmond,[7] A. Dion,[60] D. Dixit,[60] V. Doomra,[60] J. H. Do,[68] A. Drees,[60] K. A. Drees,[6] J. M. Durham,[34] A. Durum,[22] H. En'yo,[54] A. Enokizono,[54,56] R. Esha,[60] B. Fadem,[42] W. Fan,[60] N. Feege,[60] D. E. Fields,[45] M. Finger, Jr.,[9] M. Finger,[9] D. Firak,[14,60] D. Fitzgerald,[40] S. L. Fokin,[31] J. E. Frantz,[48] A. Franz,[7] A. D. Frawley,[18] Y. Fukuda,[64] P. Gallus,[13] C. Gal,[60] P. Garg,[3,60] H. Ge,[60] M. Giles,[60] F. Giordano,[23] Y. Goto,[54,55] N. Grau,[2] S. V. Greene,[65] M. Grosse Perdekamp,[23] T. Gunji,[10] H. Guragain,[19] T. Hachiya,[43,54,55] J. S. Haggerty,[7] K. I. Hahn,[16] H. Hamagaki,[10] H. F. Hamilton,[1] J. Hanks,[60] S. Y. Han,[16,30] M. Harvey,[62] S. Hasegawa,[27] T. O. S. Haseler,[19] T. K. Hemmick,[60] X. He,[19] J. C. Hill,[26] K. Hill,[11] A. Hodges,[19,23] R. S. Hollis,[8] K. Homma,[20] B. Hong,[30] T. Hoshino,[20] N. Hotvedt,[26] J. Huang,[7] K. Imai,[27] M. Inaba,[64] A. Iordanova,[8] D. Isenhower,[1] D. Ivanishchev,[52] B. V. Jacak,[60] M. Jezghani,[19] X. Jiang,[34] Z. Ji,[60] B. M. Johnson,[7,19] D. Jouan,[50] D. S. Jumper,[23] J. H. Kang,[68] D. Kapukchyan,[8] S. Karthas,[60] D. Kawall,[38] A. V. Kazantsev,[31] V. Khachatryan,[60] A. Khanzadeev,[52] A. Khatiwada,[34] C. Kim,[8,30] E.-J. Kim,[28] M. Kim,[58] T. Kim,[16] D. Kincses,[15] A. Kingan,[60] E. Kistenev,[7] J. Klatsky,[18] P. Kline,[60] T. Koblesky,[11] D. Kotov,[52,57] L. Kovacs,[15] S. Kudo,[64] B. Kurgyis,[15,60] K. Kurita,[56] Y. Kwon,[68] J. G. Lajoie,[26] D. Larionova,[57] A. Lebedev,[26] S. Lee,[68] S. H. Lee,[26,40,60] M. J. Leitch,[34] Y. H. Leung,[60] N. A. Lewis,[40] S. H. Lim,[34,53,68] M. X. Liu,[34] X. Li,[34] V.-R. Loggins,[23] D. A. Loomis,[40] K. Lovasz,[14] D. Lynch,[7] S. Lökös,[15] T. Majoros,[14] Y. I. Makdisi,[6] M. Makek,[69] V. I. Manko,[31] E. Mannel,[7] M. McCumber,[34] P. L. McGaughey,[34] D. McGlinchey,[11,34] C. McKinney,[23] M. Mendoza,[8] A. C. Mignerey,[37] A. Milov,[66] D. K. Mishra,[4] J. T. Mitchell,[7] M. Mitrankova,[57] Iu. Mitrankov,[57] G. Mitsuka,[29,55] S. Miyasaka,[54,63] S. Mizuno,[54,64] M. M. Mondal,[60] P. Montuenga,[23] T. Moon,[30,68] D. P. Morrison,[7] A. Muhammad,[41] B. Mulilo,[30,54,70] T. Murakami,[32,54] J. Murata,[54,56] K. Nagai,[63] K. Nagashima,[20] T. Nagashima,[56] J. L. Nagle,[11] M. I. Nagy,[15] I. Nakagawa,[54,55] K. Nakano,[54,63] C. Nattrass,[61] S. Nelson,[17] T. Niida,[64] R. Nouicer,[7,55] N. Novitzky,[60,64] T. Novák,[39,67] G. Nukazuka,[54,55] A. S. Nyanin,[31] E. O'Brien,[7] C. A. Ogilvie,[26] J. Oh,[53] J. D. Orjuela Koop,[11] M. Orosz,[14] J. D. Osborn,[7,40,49] A. Oskarsson,[35] G. J. Ottino,[45] K. Ozawa,[29,64] V. Pantuev,[24] V. Papavassiliou,[46] J. S. Park,[58] S. Park,[41,54,58,60] M. Patel,[26] S. F. Pate,[46] W. Peng,[65] D. V. Perepelitsa,[7,11] G. D. N. Perera,[46] D. Yu. Peressounko,[31] C. E. PerezLara,[60] J. Perry,[26] R. Petti,[7] M. Phipps,[7,23] C. Pinkenburg,[7] R. P. Pisani,[7] M. Potekhin,[7] A. Pun,[48] M. L. Purschke,[7] P. V. Radzevich,[57] N. Ramasubramanian,[60] K. F. Read,[49,61] D. Reynolds,[59] V. Riabov,[44,52] Y. Riabov,[52,57] D. Richford,[5] T. Rinn,[23,26] S. D. Rolnick,[8] M. Rosati,[26] Z. Rowan,[5] J. Runchey,[26] A. S. Safonov,[57] T. Sakaguchi,[7] H. Sako,[27] V. Samsonov,[44,52] M. Sarsour,[19] S. Sato,[27] B. Schaefer,[65] B. K. Schmoll,[61] K. Sedgwick,[8] R. Seidl,[54,55] A. Sen,[26,61] R. Seto,[8] A. Sexton,[37] D. Sharma,[60] I. Shein,[22] M. Shibata,[43] T.-A. Shibata,[54,63] K. Shigaki,[20] M. Shimomura,[26,43] T. Shioya,[64] Z. Shi,[34] P. Shukla,[4] A. Sickles,[23] C. L. Silva,[34] D. Silvermyr,[35] B. K. Singh,[3] C. P. Singh,[3] V. Singh,[3] M. Slunečka,[9] K. L. Smith,[18] M. Snowball,[34] R. A. Soltz,[33] W. E. Sondheim,[34] S. P. Sorensen,[61] I. V. Sourikova,[7] P. W. Stankus,[49] S. P. Stoll,[7] T. Sugitate,[20] A. Sukhanov,[7] T. Sumita,[54] J. Sun,[60] Z. Sun,[14] J. Sziklai,[67] R. Takahama,[43] K. Tanida,[27,55,58] M. J. Tannenbaum,[7] S. Tarafdar,[65,66] A. Taranenko,[44,59] G. Tarnai,[14] R. Tieulent,[19,36] A. Timilsina,[26] T. Todoroki,[54,55,64] M. Tomášek,[13] C. L. Towell,[1] R. S. Towell,[1] I. Tserruya,[66] Y. Ueda,[20] B. Ujvari,[14] H. W. van Hecke,[34] J. Velkovska,[65] M. Virius,[13] V. Vrba,[13,25] N. Vukman,[69] X. R. Wang,[46,55] Z. Wang,[5] Y. S. Watanabe,[10] C. P. Wong,[19,34] C. L. Woody,[7] L. Xue,[19] C. Xu,[46] Q. Xu,[65] S. Yalcin,[60] Y. L. Yamaguchi,[60] H. Yamamoto,[64] A. Yanovich,[22] I. Yoon,[58] J. H. Yoo,[30] I. E. Yushmanov,[31] H. Yu,[46,51] W. A. Zajc,[12] A. Zelenski,[6] and L. Zou[8]

(PHENIX Collaboration)

[1]*Abilene Christian University, Abilene, Texas 79699, USA*
[2]*Department of Physics, Augustana University, Sioux Falls, South Dakota 57197, USA*
[3]*Department of Physics, Banaras Hindu University, Varanasi 221005, India*
[4]*Bhabha Atomic Research Centre, Bombay 400 085, India*
[5]*Baruch College, City University of New York, New York, New York, 10010, USA*
[6]*Collider-Accelerator Department, Brookhaven National Laboratory, Upton, New York 11973-5000, USA*
[7]*Physics Department, Brookhaven National Laboratory, Upton, New York 11973-5000, USA*

[8]University of California-Riverside, Riverside, California 92521, USA
[9]Charles University, Faculty of Mathematics and Physics, 180 00 Troja, Prague, Czech Republic
[10]Center for Nuclear Study, Graduate School of Science, University of Tokyo, 7-3-1 Hongo, Bunkyo, Tokyo 113-0033, Japan
[11]University of Colorado, Boulder, Colorado 80309, USA
[12]Columbia University, New York, New York 10027 and Nevis Laboratories, Irvington, New York 10533, USA
[13]Czech Technical University, Zikova 4, 166 36 Prague 6, Czech Republic
[14]Debrecen University, H-4010 Debrecen, Egyetem tér 1, Hungary
[15]ELTE, Eötvös Loránd University, H-1117 Budapest, Pázmány P. s. 1/A, Hungary
[16]Ewha Womans University, Seoul 120-750, Korea
[17]Florida A&M University, Tallahassee, Florida 32307, USA
[18]Florida State University, Tallahassee, Florida 32306, USA
[19]Georgia State University, Atlanta, Georgia 30303, USA
[20]Physics Program and International Institute for Sustainability with Knotted Chiral Meta Matter (SKCM2), Hiroshima University, Higashi-Hiroshima, Hiroshima 739-8526, Japan
[21]Department of Physics and Astronomy, Howard University, Washington, DC 20059, USA
[22]IHEP Protvino, State Research Center of Russian Federation, Institute for High Energy Physics, Protvino, 142281, Russia
[23]University of Illinois at Urbana-Champaign, Urbana, Illinois 61801, USA
[24]Institute for Nuclear Research of the Russian Academy of Sciences, prospekt 60-letiya Oktyabrya 7a, Moscow 117312, Russia
[25]Institute of Physics, Academy of Sciences of the Czech Republic, Na Slovance 2, 182 21 Prague 8, Czech Republic
[26]Iowa State University, Ames, Iowa 50011, USA
[27]Advanced Science Research Center, Japan Atomic Energy Agency, 2-4 Shirakata Shirane, Tokai-mura, Naka-gun, Ibaraki-ken 319-1195, Japan
[28]Jeonbuk National University, Jeonju, 54896, Korea
[29]KEK, High Energy Accelerator Research Organization, Tsukuba, Ibaraki 305-0801, Japan
[30]Korea University, Seoul 02841, Korea
[31]National Research Center "Kurchatov Institute", Moscow 123098 Russia
[32]Kyoto University, Kyoto 606-8502, Japan
[33]Lawrence Livermore National Laboratory, Livermore, California 94550, USA
[34]Los Alamos National Laboratory, Los Alamos, New Mexico 87545, USA
[35]Department of Physics, Lund University, Box 118, SE-221 00 Lund, Sweden
[36]IPNL, CNRS/IN2P3, Univ Lyon, Université Lyon 1, F-69622, Villeurbanne, France
[37]University of Maryland, College Park, Maryland 20742, USA
[38]Department of Physics, University of Massachusetts, Amherst, Massachusetts 01003-9337, USA
[39]MATE, Laboratory of Femtoscopy, Károly Róbert Campus, H-3200 Gyöngyös, Mátraiút 36, Hungary
[40]Department of Physics, University of Michigan, Ann Arbor, Michigan 48109-1040, USA
[41]Mississippi State University, Mississippi State, Mississippi 39762, USA
[42]Muhlenberg College, Allentown, Pennsylvania 18104-5586, USA
[43]Nara Women's University, Kita-uoya Nishi-machi Nara 630-8506, Japan
[44]National Research Nuclear University, MEPhI, Moscow Engineering Physics Institute, Moscow 115409, Russia
[45]University of New Mexico, Albuquerque, New Mexico 87131, USA
[46]New Mexico State University, Las Cruces, New Mexico 88003, USA
[47]Physics and Astronomy Department, University of North Carolina at Greensboro, Greensboro, North Carolina 27412, USA
[48]Department of Physics and Astronomy, Ohio University, Athens, Ohio 45701, USA
[49]Oak Ridge National Laboratory, Oak Ridge, Tennessee 37831, USA
[50]IPN-Orsay, Univ. Paris-Sud, CNRS/IN2P3, Université Paris-Saclay, BP1, F-91406, Orsay, France
[51]Peking University, Beijing 100871, People's Republic of China
[52]PNPI, Petersburg Nuclear Physics Institute, Gatchina, Leningrad region, 188300, Russia
[53]Pusan National University, Pusan 46241, Korea
[54]RIKEN Nishina Center for Accelerator-Based Science, Wako, Saitama 351-0198, Japan
[55]RIKEN BNL Research Center, Brookhaven National Laboratory, Upton, New York 11973-5000, USA
[56]Physics Department, Rikkyo University, 3-34-1 Nishi-Ikebukuro, Toshima, Tokyo 171-8501, Japan
[57]Saint Petersburg State Polytechnic University, St. Petersburg, 195251 Russia
[58]Department of Physics and Astronomy, Seoul National University, Seoul 151-742, Korea

[59]Chemistry Department, Stony Brook University, SUNY, Stony Brook, New York 11794-3400, USA
[60]Department of Physics and Astronomy, Stony Brook University, SUNY, Stony Brook, New York 11794-3800, USA
[61]University of Tennessee, Knoxville, Tennessee 37996, USA
[62]Texas Southern University, Houston, Texas 77004, USA
[63]Department of Physics, Tokyo Institute of Technology, Oh-okayama, Meguro, Tokyo 152-8551, Japan
[64]Tomonaga Center for the History of the Universe, University of Tsukuba, Tsukuba, Ibaraki 305, Japan
[65]Vanderbilt University, Nashville, Tennessee 37235, USA
[66]Weizmann Institute, Rehovot 76100, Israel
[67]Institute for Particle and Nuclear Physics, Wigner Research Centre for Physics, Hungarian Academy of Sciences (Wigner RCP, RMKI) H-1525 Budapest 114, POBox 49, Budapest, Hungary
[68]Yonsei University, IPAP, Seoul 120-749, Korea
[69]Department of Physics, Faculty of Science, University of Zagreb, Bijenička c. 32 HR-10002 Zagreb, Croatia
[70]Department of Physics, School of Natural Sciences, University of Zambia, Great East Road Campus, Box 32379, Lusaka, Zambia

(Received 14 March 2023; accepted 9 May 2023; published 9 June 2023)

Presented are the first measurements of the transverse single-spin asymmetries ($A_N$) for neutral pions and eta mesons in $p + \mathrm{Au}$ and $p + \mathrm{Al}$ collisions at $\sqrt{s_{NN}} = 200$ GeV in the pseudorapidity range $|\eta| < 0.35$ with the PHENIX detector at the Relativistic Heavy Ion Collider. The asymmetries are consistent with zero, similar to those for midrapidity neutral pions and eta mesons produced in $p + p$ collisions. These measurements show no evidence of additional effects that could potentially arise from the more complex partonic environment present in proton-nucleus collisions.

DOI: 10.1103/PhysRevD.107.112004

## I. INTRODUCTION

Transverse single-spin asymmetries (TSSAs) in particle production for hadronic collisions involving a transversely polarized proton result from nonperturbative spin-momentum correlations in the proton and/or the process of hadronization [1]. For recent discussions of TSSAs measured in polarized $p + p$ collisions at the Relativistic Heavy Ion Collider (RHIC) and the possible mechanisms contributing to them, see Refs. [2–10].

In hadronic collisions involving a nucleus, the underlying partonic origins of the asymmetries could be affected by the presence of more complex quantum-chromodynamics environments. For example, relations between TSSAs and the physics of small parton momentum fractions have been proposed, in particular, how comparisons of asymmetries measured in $p^{\uparrow} + p$ and $p^{\uparrow} + A$ collisions for forward hadron production could be used to probe gluon saturation effects in the nucleus [11]. Further theoretical works have explored these ideas [12–22]. At RHIC, TSSA measurements for proton-nucleus collisions have been performed for forward charged hadrons [23,24] and forward $J/\psi$ mesons [25] by PHENIX, and for forward $\pi^0$ production by STAR [26], revealing some nuclear dependencies that remain to be understood in detail. PHENIX has additionally measured the TSSAs for far forward neutron production, with the observed nuclear dependence of the asymmetries understood to be due to the interplay of hadronic and electromagnetic interactions in ultraperipheral collisions [27,28]. No experimental measurements exist, and very little theoretical work has been done to explore possible nuclear effects for midrapidity TSSA observables, which can only be studied at RHIC.

## II. ANALYSIS

This brief article reports the first measurement of the TSSAs of neutral pions and eta mesons in proton-Gold ($p^{\uparrow} + \mathrm{Au}$) and proton-Aluminum ($p^{\uparrow} + \mathrm{Al}$) collisions at $\sqrt{s_{NN}} = 200$ GeV at midrapidity ($|\eta| < 0.35$). The data were taken in 2015 at RHIC, and total integrated luminosities of approximately 202 and 690 $\mathrm{nb}^{-1}$, respectively, were collected.

Measurements were performed with collisions of a vertically polarized proton beam on an ion beam (Au or Al). The proton or ion bunches are separated by 106 ns in the RHIC rings. Each polarized proton bunch is assigned a

*Deceased.
†PHENIX Spokesperson; akiba@rcf.rhic.bnl.gov

polarization direction, either up or down, so that measurements with both spin directions can be performed nearly simultaneously. This significantly reduces any possible systematic uncertainties related to the detector performance with time. The average proton beam polarization was 0.60 and 0.57 in $p^{\uparrow}+\mathrm{Au}$ and $p^{\uparrow}+\mathrm{Al}$ collisions, respectively [29], with a relative uncertainty of 3% due to uncertainty in polarization normalization.

The data analysis procedure follows almost exactly from the recent TSSA measurement for $\pi^0$ and $\eta$ mesons in $\sqrt{s}=200$ GeV polarized $p+p$ collisions [5], with the distinction that only the proton beam is polarized in $p^{\uparrow}+A$ collisions. Only events with a collision $z$ vertex within $\pm 30$ cm from the nominal collision point were selected. The collision or minimum-bias trigger, as well as vertex position, were determined by two beam-beam counters (BBC) located at $\pm 144$ cm from the nominal collision point along the beam line, and covering the pseudorapidity range $3.1<|\eta|<3.9$ with full azimuthal coverage.

Neutral pions and eta mesons were reconstructed through their two-photon decay in the electromagnetic calorimeters (EMCal) of PHENIX. The EMCal is located in two nearly back-to-back central arm spectrometers (west and east), each covering $\Delta\phi=\pi/2$ in azimuth and $\pm 0.35$ in pseudorapidity. The EMCal comprises two types of calorimeters, six sectors of sampling lead-scintillator (PbSc) calorimeters and two sectors of Čerenkov lead-glass (PbGl) calorimeters [30]. The two-calorimeter systems have different granularity ($\Delta\phi\times\Delta\eta=0.011\times 0.011$ in PbSc and $0.008\times 0.008$ in PbGl) and also have a different response to charged hadrons, which provides important systematic cross checks for the measurement.

The PHENIX EMCal was also used to generate a high-$p_T$ photon trigger to tag events with a high-energy cluster in the EMCal. The high-$p_T$ photon trigger (with an energy threshold of 1.5 GeV) in coincidence with a minimum-bias trigger that requires charged particles in both BBC detectors was used to collect the $\pi^0$ and $\eta$ statistics in this analysis. The efficiency of such a trigger for $\pi^0$ 's increased from 20% at $p_T=3$ GeV/$c$ to 90% at $p_T>6$ GeV/$c$, with the plateaued efficiency level defined by the acceptance of the live trigger tiles.

Photons were identified in the EMCal by placing selection criteria on the shower profile and time of flight (TOF) with $|\mathrm{TOF}|<5$ ns, and with a minimum energy selection of 0.5 GeV to reduce the contribution from electronic noise in the EMCal, and combinatorial background in $\pi^0$ and $\eta$ reconstruction. A charged track veto was also implemented to eliminate clusters that are geometrically associated with a track and to suppress the background from electrons and charged hadrons. Photon pairs were reconstructed by finding a high-$p_T$ trigger photon and pairing it with another photon from the same event and spectrometer arm. Photon pairs passing an energy-asymmetry requirement, $\alpha=|E_1-E_2|/(E_1+E_2)<0.8$, were selected for further analysis.

Figure 1 shows the two-photon invariant mass distributions around the $\pi^0$ and $\eta$ peaks for photon pairs within $4<p_T<5$ GeV/$c$ in the west central arm spectrometer for $p+\mathrm{Au}$ and $p+\mathrm{Al}$ collisions. The $\pi^0$ and $\eta$ meson yields were defined to be within the signal-invariant mass window (blue leftward-hatched regions in Fig. 1) of $\pm 25$ and $\pm 70$ MeV/$c^2$ from the $\pi^0$ and $\eta$ mass peaks, respectively, in the two-photon invariant mass distribution for each $p_T$ bin. The sideband regions used to approximate the combinatorial background under the signal peak (red rightward-hatched regions in Fig. 1) are defined as 47–97 and 177–227 MeV/$c^2$ for the $\pi^0$ and 300–400 and 700–800 MeV/$c^2$ for the $\eta$ mesons. The same signal and sideband regions were used in a previous PHENIX analysis [5]. The combinatorial background for the two-photon invariant mass spectrum (described by a third-order polynomial and shown as the green solid lines in Fig. 1) was used to quantify the fraction of background existing under the signal peaks. For the $\pi^0$, this ranged from 14% (13%) to 6% (6%) from the lowest to the highest $p_T$ bins in $p+\mathrm{Au}$ ($p+\mathrm{Al}$) collisions, while for the $\eta$, the combinatorial background under the signal peak ranged from 79% (77%) to 48% (43%) in $p+\mathrm{Au}$ ($p+\mathrm{Al}$) collisions.

Similar to the recent $p+p$ $\pi^0$ and $\eta$ TSSA analysis [5], the transverse single-spin asymmetry $A_N$ is determined with the "relative-luminosity" formula, which is calculated separately for the two detector arms. This yields measurements from two independent data sets that are verified for consistency and then averaged to obtain the final result. The equation for the relative-luminosity TSSA is

$$A_N=\frac{1}{P\langle\cos(\phi)\rangle}\frac{N^{\uparrow}-\mathcal{R}N^{\downarrow}}{N^{\uparrow}+\mathcal{R}N^{\downarrow}}, \tag{1}$$

where $P$ is the beam polarization, and $\mathcal{R}$ is the relative luminosity, defined as the ratio of integrated luminosities between the bunches with $\uparrow$ and $\downarrow$ spin states and measured by the BBC detectors. Here, $\langle\cos(\phi)\rangle$ is the acceptance factor which reflects the detector azimuthal coverage, calculated separately for each $p_T$ bin and spectrometer arm, and $N$ refers to the yields, with the arrows referring to the up ($\uparrow$) or down ($\downarrow$) polarization of the proton beam.

Another method to calculate the asymmetry is the "square-root" formula, which is used as a cross check. The square-root formula is defined as

$$A_N=\frac{1}{P\langle\cos(\phi)\rangle}\frac{\sqrt{N_L^{\uparrow}N_R^{\downarrow}}-\sqrt{N_L^{\downarrow}N_R^{\uparrow}}}{\sqrt{N_L^{\uparrow}N_R^{\downarrow}}+\sqrt{N_L^{\downarrow}N_R^{\uparrow}}}, \tag{2}$$

and it is used to calculate the asymmetry for both spectrometer arms simultaneously, where the $L$ and $R$

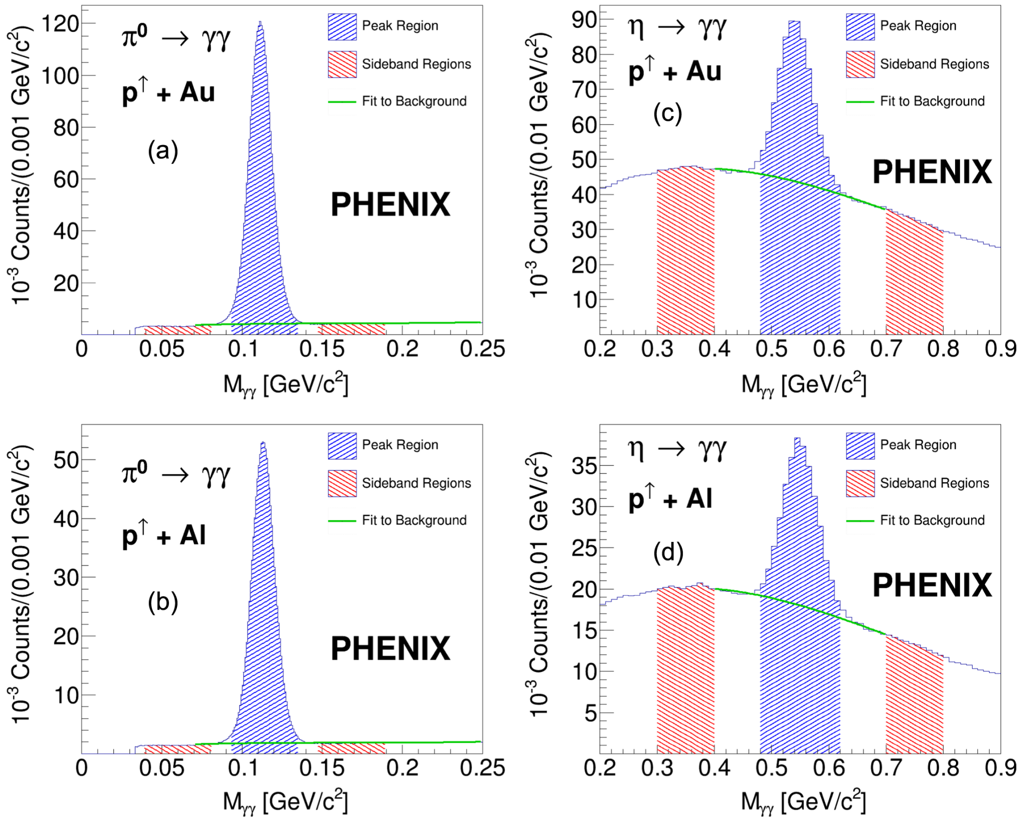


FIG. 1. Invariant mass distributions around the $\pi^0 \to \gamma\gamma$ peak in (a) $p^\uparrow + \mathrm{Au}$ collisions and (b) $p^\uparrow + \mathrm{Al}$ collisions and around the $\eta \to \gamma\gamma$ peak in (c) $p^\uparrow + \mathrm{Au}$ collisions and (d) $p^\uparrow + \mathrm{Al}$ collisions for photon pairs within $4 < p_T[\mathrm{GeV}/c] < 5$ in the west central-arm spectrometer. The blue leftward-hatched regions are the signal peaks, used for quantifying yields for the $A_N$ calculations; the red rightward-hatched regions are the sidebands, used to quantify yields for the $A_N^{\mathrm{BG}}$ calculations; and the green solid curves correspond to fits to the combinatorial background, used in calculating the background fractions.

subscripts of $N$ correspond to yields measured in the left and right detector arms, respectively, with respect to the polarized-proton-going direction. This results in only one measurement of $A_N$ that can be compared with the weighted average of the left and right relative-luminosity asymmetry calculation. The comparison of results using Eqs. (1) and (2) was used as a cross check, with corresponding systematic uncertainties discussed below.

As an additional cross check, the TSSA is calculated as a function of $\phi$, in which case, a cosine modulation is fit to extract the asymmetry. This was found to be statistically consistent with the main asymmetry results.

The measured asymmetries were corrected for the background as follows,

$$A_N^{\mathrm{sig}} = \frac{A_N - r \cdot A_N^{\mathrm{BG}}}{1 - r}, \tag{3}$$

where $r$ is the background fraction under the $\pi^0$ or $\eta$ peaks, calculated from the background fits (green solid lines) shown in Fig. 1. Note that $A_N^{\mathrm{BG}}$ is the background asymmetry, which was evaluated from the sidebands on both sides of the $\pi^0$ and $\eta$ peaks, also shown in Fig. 1. The background asymmetry is consistent with zero in all $p_T$ bins and all collision systems for both the $\pi^0$ and $\eta$ mesons.

Asymmetries were calculated separately for each accelerator fill, during which the detector performance and beam conditions are considered to be relatively stable. The final asymmetry was obtained from the weighted average over the accelerator fills.

The possible sources of systematic uncertainties considered are (i) the background contribution $r$ in Eq. (3), and (ii) possible variation in detector performance and beam conditions. A systematic uncertainty on the background fraction is quantified by varying the fit ranges used to calculate $r$ and computing how much the background-corrected asymmetry changes. The variations in detector performance and beam conditions, including uncertainty on the relative luminosity, were tested by comparing results calculated with the "relative-luminosity formula" Eq. (1) and the "square-root formula" Eq. (2), and with a technique known as "bunch shuffling" [31]. The asymmetries calculated with the different formulas were found to be statistically consistent when taking into account the correlation between data sets. However, a conservative systematic uncertainty calculated as the absolute value of

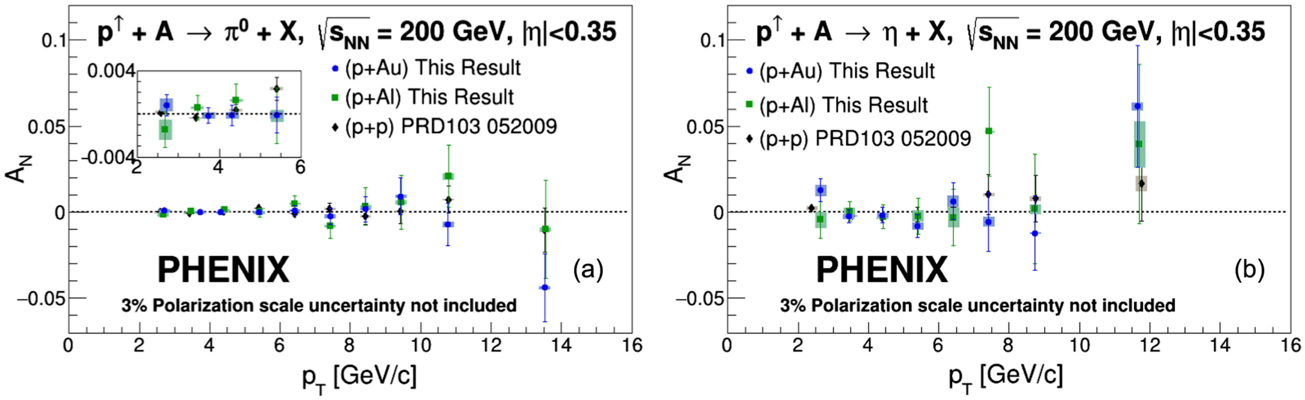


FIG. 2. Transverse single-spin asymmetry for (a) $\pi^0$ and (b) $\eta$ mesons in $p^\uparrow + \mathrm{Au}$ collisions (blue circles), and $p^\uparrow + \mathrm{Al}$ collisions (green squares) from this measurement, shown alongside the same measurement in polarized $p + p$ collisions from Ref. [5] (black diamonds). The error bars represent the statistical uncertainty ($\sigma^{\mathrm{stat}}$) while the boxes represent the total systematic uncertainty ($\sigma^{\mathrm{syst}}$).

the difference in central values is assigned. In the bunch-shuffling procedure, the polarization of each bunch is randomly assigned to be up or down, and a distribution of $A_N$ in each $p_T$ bin is obtained by repeating the procedure 10,000 times [31]. While most $p_T$ bins were found to be consistent with the statistical variation, some of the lower $p_T$ bins for both the $\pi^0$ and the $\eta$ in both $p + A$ collision systems included up to 15% variation beyond what was expected from statistical fluctuations. To account for this effect, an additional systematic uncertainty was assigned in any $p_T$ bin showing variations significantly beyond expected statistical fluctuations.

## III. RESULTS AND DISCUSSION

Figure 2 shows the measurement of $A_N$ for $\pi^0$ and $\eta$ mesons in $p^\uparrow + \mathrm{Au}$ and $p^\uparrow + \mathrm{Al}$ collisions at $\sqrt{s_{NN}} = 200$ GeV. The measured asymmetries in $p^\uparrow + \mathrm{Au}$ and $p^\uparrow + \mathrm{Al}$ are consistent with zero across the entire $p_T$ range for both the $\pi^0$ and $\eta$ mesons. Table I lists the asymmetries, statistical uncertainties, and total systematic uncertainties for the $\pi^0$ and $\eta$ mesons in $p^\uparrow + \mathrm{Au}$ and $p^\uparrow + \mathrm{Al}$ collisions.

The TSSA measurements presented here probe the complex dynamics of partons within a nucleus. Measurements of asymmetries with heavy nuclei have not been

TABLE I. Summary of final asymmetries with statistical and systematic uncertainties for $\pi^0$ and $\eta$ mesons in $p^\uparrow + A$ collisions. Note that $\sigma^{\mathrm{syst}}$ corresponds to the systematic uncertainties, displayed by the shaded boxes in Fig. 2.

| Meson | Collisions | $p_T$ range [GeV/c] | $\langle p_T \rangle$[GeV/$c$] | $A_N$ | $\sigma^{\mathrm{stat}}$ | $\sigma^{\mathrm{syst}}$ |
|---|---|---|---|---|---|---|
| $\pi^0$ | $p^\uparrow + \mathrm{Au}$ | 2–3 | 2.71 | 0.000818 | 0.000993 | 0.000569 |
| | | 3–4 | 3.73 | −0.000145 | 0.000701 | 0.000286 |
| | | 4–5 | 4.31 | −0.000135 | 0.000974 | 0.000257 |
| | | 5–6 | 5.4 | −0.00011 | 0.00164 | 0.00028 |
| | | 6–7 | 6.41 | 0.00097 | 0.00281 | 0.00024 |
| | | 7–8 | 7.42 | −0.00243 | 0.00464 | 0.00109 |
| | | 8–9 | 8.43 | 0.00179 | 0.00732 | 0.00055 |
| | | 9–10 | 9.44 | 0.0093 | 0.0106 | 0.0005 |
| | | 10–12 | 10.8 | −0.0072 | 0.0122 | 0.0014 |
| | | 12–20 | 13.5 | −0.0438 | 0.0198 | 0.0008 |
| $\pi^0$ | $p^\uparrow + \mathrm{Al}$ | 2–3 | 2.67 | −0.00147 | 0.00163 | 0.00088 |
| | | 3–4 | 3.47 | 0.00056 | 0.00113 | 0.00006 |
| | | 4–5 | 4.41 | 0.00126 | 0.00153 | 0.00005 |
| | | 5–6 | 5.41 | −0.00018 | 0.00254 | 0.00051 |
| | | 6–7 | 6.42 | 0.00500 | 0.00429 | 0.00042 |
| | | 7–8 | 7.42 | −0.00809 | 0.00699 | 0.00060 |
| | | 8–9 | 8.43 | 0.0035 | 0.0109 | 0.0004 |

*(Table continued)*

TABLE I. *(Continued)*

| Meson | Collisions | $p_T$ range [GeV/c] | $\langle p_T \rangle$[GeV/$c$] | $A_N$ | $\sigma^{\text{stat}}$ | $\sigma^{\text{syst}}$ |
|---|---|---|---|---|---|---|
| | | 9–10 | 9.44 | 0.0058 | 0.0155 | 0.0010 |
| | | 10–12 | 10.8 | 0.0208 | 0.0181 | 0.0016 |
| | | 12–20 | 13.6 | −0.0099 | 0.0286 | 0.0011 |
| $\eta$ | $p^{\uparrow}+\text{Au}$ | 2–3 | 2.64 | 0.01279 | 0.00665 | 0.00306 |
| | | 3–4 | 3.44 | −0.00255 | 0.00377 | 0.00115 |
| | | 4–5 | 4.41 | −0.00168 | 0.00448 | 0.00117 |
| | | 5–6 | 5.4 | −0.00810 | 0.00667 | 0.00183 |
| | | 6–7 | 6.41 | 0.0064 | 0.0108 | 0.0029 |
| | | 7–8 | 7.42 | −0.0056 | 0.0170 | 0.0026 |
| | | 8–10 | 8.74 | −0.0122 | 0.0216 | 0.0002 |
| | | 10–20 | 11.7 | 0.0615 | 0.0351 | 0.0021 |
| $\eta$ | $p^{\uparrow}+\text{Al}$ | 2–3 | 2.64 | −0.0044 | 0.0107 | 0.0046 |
| | | 3–4 | 3.46 | 0.00043 | 0.00575 | 0.00219 |
| | | 4–5 | 4.42 | −0.00278 | 0.00686 | 0.00050 |
| | | 5–6 | 5.41 | −0.0022 | 0.0104 | 0.0031 |
| | | 6–7 | 6.42 | −0.0032 | 0.0163 | 0.0055 |
| | | 7–8 | 7.42 | 0.0468 | 0.0260 | 0.0004 |
| | | 8–10 | 8.74 | 0.0017 | 0.0318 | 0.0027 |
| | | 10–20 | 11.7 | 0.0395 | 0.0464 | 0.0133 |

performed at collider energies before 2015. Therefore, it is unclear to what extent the nuclear environment affects TSSAs. Collisions with a nucleus explore spin-momentum correlations in an environment where larger multiplicities and stronger color fields could play an additional role. In a factorized picture, initial-state spin-momentum correlations in the polarized proton cannot be affected by the presence of a nucleus; however, it is possible for final-state spin-momentum correlations in the process of hadronization to be affected as the scattered parton passes through the nuclear matter. Allowing for factorization-breaking effects, the larger color field of the nuclear remnant in $p^{\uparrow}+A$ collisions as compared to the proton remnant in $p^{\uparrow}+p$ collisions could potentially modify the observed asymmetries [32,33]. Neutral-pion measurements in the forward region [26] and charged-hadron measurements in the intermediate rapidity region [23,24] show sizable TSSAs in $p^{\uparrow}+p$ collisions, with moderate nuclear modifications in $p^{\uparrow}+A$ for the former and strong nuclear modifications in $p^{\uparrow}+A$ for the latter. In contrast, the $\pi^0$ and $\eta$ meson asymmetries at midrapidity are consistent with zero in all collision systems, showing no difference between $p^{\uparrow}+p$ and $p^{\uparrow}+A$ collisions.

## IV. SUMMARY

The data presented here were motivated by the outstanding questions regarding the physical origin of transverse single-spin asymmetries. The TSSAs of midrapidity $\pi^0$ and $\eta$ mesons were measured in $p^{\uparrow}+\text{Au}$ and $p^{\uparrow}+\text{Al}$ collisions at $\sqrt{s_{NN}}=200$ GeV by the PHENIX experiment at RHIC. The measured asymmetries are consistent with zero up to very high precision in both collision systems for both meson species. The data presented here will contribute to the understanding of transverse spin phenomena in the more complex environment present in proton-nucleus collisions. In particular, we find that at midrapidity the presence of a heavy nucleus in the collision does not significantly modify the magnitude of the measured TSSAs.

## ACKNOWLEDGMENTS

We thank the staff of the Collider-Accelerator and Physics Departments at Brookhaven National Laboratory and the staff of the other PHENIX participating institutions for their vital contributions. We acknowledge support from the Office of Nuclear Physics in the Office of Science of the Department of Energy, the National Science Foundation, Abilene Christian University Research Council, Research Foundation of SUNY, and Dean of the College of Arts and Sciences, Vanderbilt University (USA), Ministry of Education, Culture, Sports, Science, and Technology and the Japan Society for the Promotion of Science (Japan), Natural Science Foundation of China (People's Republic of China), Croatian Science Foundation and Ministry of Science and Education (Croatia), Ministry of Education, Youth and Sports (Czech Republic), Centre National de la Recherche Scientifique, Commissariat à l'Énergie Atomique, and Institut National de Physique Nucléaire et de Physique des Particules (France), the J. Bolyai Research Scholarship, EFOP, the New National Excellence Program (ÚNKP), NKFIH, and OTKA (Hungary), Department of Atomic Energy and Department of Science and Technology (India), Israel Science Foundation (Israel), Basic Science Research and SRC(CENuM) Programs through NRF funded by the Ministry of Education and the Ministry of Science and ICT (Korea), Ministry of Education and Science, Russian Academy of Sciences, Federal Agency of Atomic Energy (Russia), VR and Wallenberg Foundation (Sweden), University of Zambia, the Government of the Republic of Zambia (Zambia), the US Civilian Research and Development Foundation for the Independent States of the Former Soviet Union, the Hungarian American Enterprise Scholarship Fund, the US-Hungarian Fulbright Foundation, and the US-Israel Binational Science Foundation.

[1] M. Anselmino, A. Mukherjee, and A. Vossen, Transverse spin effects in hard semi-inclusive collisions, Prog. Part. Nucl. Phys. **114**, 103806 (2020).

[2] U. Acharya *et al.* (PHENIX Collaboration), Improving constraints on gluon spin-momentum correlations in transversely polarized protons via midrapidity open-heavy-flavor electrons in $p^{\uparrow}+p$ collisions at $\sqrt{s}=200$ GeV, Phys. Rev. D **107**, 052012 (2023).

[3] U. Acharya *et al.* (PHENIX Collaboration), Transverse-single-spin asymmetries of charged pions at midrapidity in transversely polarized $p+p$ collisions at $\sqrt{s}=200$ GeV, Phys. Rev. D **105**, 032003 (2022).

[4] U. Acharya *et al.* (PHENIX Collaboration), Probing Gluon Spin-Momentum Correlations in Transversely Polarized Protons through Midrapidity Isolated Direct Photons in $p^{\uparrow}+p$ Collisions at $\sqrt{s}=200$ GeV, Phys. Rev. Lett. **127**, 162001 (2021).

[5] U. Acharya *et al.* (PHENIX Collaboration), Transverse single-spin asymmetries of midrapidity $\pi^0$ and $\eta$ mesons in polarized $p+p$ collisions at $\sqrt{s}=200$ GeV, Phys. Rev. D **103**, 052009 (2021).

[6] U. Acharya *et al.* (PHENIX Collaboration), Transverse momentum dependent forward neutron single spin asymmetries in transversely polarized $p+p$ collisions at $\sqrt{s}=200$ GeV, Phys. Rev. D **103**, 032007 (2021).

[7] M. Abdallah *et al.* (STAR Collaboration), Azimuthal transverse single-spin asymmetries of inclusive jets and identified hadrons within jets from polarized $pp$ collisions at $\sqrt{s}=200$ GeV, Phys. Rev. D **106**, 072010 (2022).

[8] J. Adam *et al.* (STAR Collaboration), Measurement of transverse single-spin asymmetries of $\pi^0$ and electromagnetic jets at forward rapidity in 200 and 500 GeV transversely polarized proton-proton collisions, Phys. Rev. D **103**, 092009 (2021).

[9] L. Adamczyk *et al.* (STAR Collaboration), Transverse spin-dependent azimuthal correlations of charged pion pairs measured in $\mathrm{p}^{\uparrow}+\mathrm{p}$ collisions at $\sqrt{s}=500$ GeV, Phys. Lett. B **780**, 332 (2018).

[10] L. Adamczyk *et al.* (STAR Collaboration), Azimuthal transverse single-spin asymmetries of inclusive jets and charged pions within jets from polarized-proton collisions at $\sqrt{s}=500$ GeV, Phys. Rev. D **97**, 032004 (2018).

[11] Z. B. Kang and F. Yuan, Single spin asymmetry scaling in the forward rapidity region at RHIC, Phys. Rev. D **84**, 034019 (2011).

[12] Y. V. Kovchegov and M. D. Sievert, A new mechanism for generating a single transverse spin asymmetry, Phys. Rev. D **86**, 034028 (2012); **86**, 079906(E) (2012).

[13] A. Schäfer and J. Zhou, Color entanglement for $\gamma$-jet production in polarized $pA$ collisions, Phys. Rev. D **90**, 094012 (2014).

[14] A. Schäfer and J. Zhou, Transverse single spin asymmetry in direct photon production in polarized $pA$ collisions, Phys. Rev. D **90**, 034016 (2014).

[15] Y. V. Kovchegov and M. D. Sievert, Calculating TMDs of a large nucleus: Quasi-classical approximation and quantum evolution, Nucl. Phys. **B903**, 164 (2016).

[16] J. Zhou, Transverse single spin asymmetry in Drell-Yan production in polarized $pA$ collisions, Phys. Rev. D **92**, 014034 (2015).

[17] Y. Hatta, B. W. Xiao, S. Yoshida, and F. Yuan, Single spin asymmetry in forward $pA$ collisions, Phys. Rev. D **94**, 054013 (2016).

[18] Y. Hatta, B. W. Xiao, S. Yoshida, and F. Yuan, Single spin asymmetry in forward $pA$ collisions II: Fragmentation contribution, Phys. Rev. D **95**, 014008 (2017).

[19] J. Zhou, Single spin asymmetries in forward $p-p/A$ collisions revisited: The role of color entanglement, Phys. Rev. D **96**, 034027 (2017).

[20] S. Benić and Y. Hatta, Single spin asymmetry in forward $pA$ collisions: Phenomenology at RHIC, Phys. Rev. D **99**, 094012 (2019).

[21] Y. V. Kovchegov and M. G. Santiago, Lensing mechanism meets small-$x$ physics: Single transverse spin asymmetry in $p^{\uparrow}+p$ and $p^{\uparrow}+A$ collisions, Phys. Rev. D **102**, 014022 (2020).

[22] S. Benić, D. Horvatić, A. Kaushik, and E. A. Vivoda, Odderon mechanism for transverse single spin asymmetry in the Wandzura-Wilczek approximation, Phys. Rev. D **106**, 114025 (2022).

[23] C. Aidala *et al.* (PHENIX Collaboration), Nuclear Dependence of the Transverse Single-Spin Asymmetry in the Production of Charged Hadrons at Forward Rapidity in Polarized $p+p$, $p+\mathrm{Al}$, and $p+\mathrm{Au}$ Collisions at $\sqrt{s_{NN}}=200$ GeV, Phys. Rev. Lett. **123**, 122001 (2019).

[24] N. J. Abdulameer *et al.* (PHENIX Collaboration), Transverse single-spin asymmetry of midrapidity charged hadrons in $p+\mathrm{Au}$ and $p+\mathrm{Al}$ collisions at $\sqrt{s_{NN}}=200$ GeV, arXiv:2303.07191.

[25] C. Aidala *et al.* (PHENIX Collaboration), Single-spin asymmetry of $J/\psi$ production in $p+p$, $p+\mathrm{Al}$, and

$p+$ Au collisions with transversely polarized proton beams at $\sqrt{s_{NN}} = 200$ GeV, Phys. Rev. D **98**, 012006 (2018).

[26] J. Adam *et al.* (STAR Collaboration), Comparison of transverse single-spin asymmetries for forward $\pi^0$ production in polarized $pp$, $p$Al and $p$Au collisions at nucleon pair c.m. energy $\sqrt{s_{\mathrm{NN}}} = 200$ GeV, Phys. Rev. D **103**, 072005 (2021).

[27] C. Aidala *et al.* (PHENIX Collaboration), Nuclear Dependence of the Transverse-Single-Spin Asymmetry for Forward Neutron Production in Polarized $p+A$ Collisions at $\sqrt{s_{NN}} = 200$ GeV, Phys. Rev. Lett. **120**, 022001 (2018).

[28] U. Acharya *et al.* (PHENIX Collaboration), Transverse single spin asymmetries of forward neutrons in $p+p$, $p+$ Al and $p+$ Au collisions at $\sqrt{s_{NN}} = 200$ GeV as a function of transverse and longitudinal momenta, Phys. Rev. D **105**, 032004 (2022).

[29] W. B. Schmidke *et al.* (The RHIC Polarimetry Group), RHIC polarization for Runs 9-17 (2018) 10.2172/1473643.

[30] L. Aphecetche *et al.* (PHENIX Collaboration), PHENIX calorimeter, Nucl. Instrum. Methods Phys. Res., Sect. A **499**, 521 (2003).

[31] A. Adare *et al.* (PHENIX Collaboration), Inclusive double-helicity asymmetries in neutral-pion and eta-meson production in $\vec{p}+\vec{p}$ collisions at $\sqrt{s} = 200$ GeV, Phys. Rev. D **90**, 012007 (2014).

[32] T. C. Rogers and P. J. Mulders, No generalized TMD-factorization in hadro-production of high transverse momentum hadrons, Phys. Rev. D **81**, 094006 (2010).

[33] T. C. Rogers, Extra spin asymmetries from the breakdown of transverse-momentum-dependent factorization in hadron-hadron collisions, Phys. Rev. D **88**, 014002 (2013).